THE ULTRAVIOLET CROSS-SECTIONS OF OZONE: I. THE MEASUREMENTS

A. M. BASS*, NBS, Washington, DC 20234
R. J. PAUR, EPA**, Research Triangle Park, NC 27711

Summary

Absorption cross-sections of ozone have been measured over the range 230 nm to 350 nm, and for temperatures 200K to 300K, with improved photometric accuracy and spectral resolution. These measurements are referred to the cross-section at the 253.65 nm mercury line, $1147 \times 10^{-20} cm^2$ (1), and show an internal consistency of ±1%.

1. Method and experimental

The determination of absorption cross-sections in systems that obey the Beer-Lambert Law is, in principle, a fairly straightforward measurement problem requiring knowledge only of path lengths, light transmittance, and sample concentration. Ozone presents a particular problem in the difficulty of characterizing accurately the sample concentration. In measurement applications the absorption of radiation at 253.65 nm is frequently used as a means of assaying the ozone content of a sample. In such applications a best estimate of the cross-section from published results has been used. The published values range from about 1136×10^{-20} to about 1162×10^{-2} cm^2, and the value reported by Hearn (1) (1147×10^{-20} cm^2) has frequently been selected as the reference value for the cross-section at 253.65 nm.

We refer all measurements to the absorption at 253.65 nm by using the Hearn value of the cross-section.

The absorption cross-sections were determined from the relation

$$n\sigma = kcL = \log_e\left(\frac{I}{Io}\right)$$

where: Io, I are the incident and transmitted radiation intensities
L is the pathlength (cm); c is the ozone concentration (atm)
k is the absorption coefficient (cm^{-1} atm^{-1})
σ is the absorption cross-section (cm^2)
n is the column density of the ozone sample (cm^{-2}).

The incident continuum radiation was produced by a DC arc in argon at atmospheric pressure (2) operating at a power of 3000 watts. The radiation from the arc was focused on the entrance slit of a 1.8 meter focal length Ebert scanning monochromator. The instrument uses a 1200 grooves/mm grating, and for the mechanical slit widths that were used in these measurements has a spectral resolution less than 0.025 nm. The monochromator is driven, through a precision screw, by a stepping motor

* Work supported in part by NASA Upper Atmosphere Program.
**Any policy issues discussed should not be construed to represent EPA policy.

that is capable of moving the grating through extremely small intervals. Wavelength steps of 0.05 nm were used to insure that the ozone absorption bands would be accurately reproduced. The wavelength scale of the instrument was calibrated between 200 and 365 nm by reference to 23 emission lines of mercury, cadmium, and zinc. The uncertainty of the wavelength determination is less than 0.025 nm. The emergent radiation from the monochromator passed through a narrow-band filter to remove stray radiation before entering the absorption cells.

The measurement of sample transmittance was made by using a novel photometric technique (Figure 1). Two pyrex absorption cells, each 1 meter long and 12mm diameter, were mounted in a double-walled chamber in which they were submerged in methanol. The exit beam from the monochromator was split by a partially aluminized reflector into two approximately equal beams that were directed through the cells. At the exit end of each cell was a photomultiplier detector. The photocurrent in each tube was converted to frequency, and the signals were connected to scalers for display and counting.

A gas handling system provided two streams: air (or oxygen) in one, and ozonized air (or oxygen) in the other. The ozone was produced either by UV photolysis or by electrical discharge in the air (or oxygen) stream. No differences were noted in the results of measurements with respect to the method of ozone production. By operating appropriate valves the flow of the ozonized air was directed alternately to each of the absorption cells. The residence time of a sample in the cells was about two seconds. Figure 2 shows how the transmittance of the ozone sample may be derived from the measurements in this system. (T_{freq} is the intensity of the beam as detected by the photomultiplier tube for each cell, where the photocurrent is converted to a frequency for digital measurement). It should be noted that the transmittance as determined by this method is equivalent to that of a single cell equal in length to the combined lengths of the two cells. Since the UV radiation source is viewed simultaneously by both photomultiplier detectors, fluctuations in the source intensity do not effect the transmittance measurement. Also, impurities in the air stream will not affect the transmittance measurement unless the impurity can react with ozone.

The uncertainty in the transmittance determination is estimated to be 2 in 10^5 arising from counting statistics.

The ozone concentration, or number density, in the sample is determined by making absorption measurements at 253.65 nm in two pairs of absorption cells (assay cells). A mercury lamp placed at one end of the assay cells is viewed by solar-blind photodiodes through narrow-band interference filters which isolate the Hg 253.65 nm line. As shown in Figure 1 the assay cells are placed at the entrance and exit of the main absorption cells and serve to indicate the degree of ozone loss in passing through the main cells. The pairs of assay cells are 1 cm and 5 cm long. These lengths allow us to make accurate concentration measurements over an ozone concentration range of 10 to 4000 ppm.

The temperature and pressure of the air/ozone mixture are measured by sensors within the sample stream. The sample temperature is varied by circulating methanol from a refrigerated reservoir into the chamber in which the absorption cells are located. Temperature control to better than 1 K can be maintained over the temperature range 198 K to 300 K. The sample temperature uncertainty is about 0.25 K; the uncertainty of the pressure measurement is about 1 mbar.

The entire measurement process and data collection and reduction are controlled by a computer. In the measurement sequence the monochromator is set at the desired wavelength and a flow pattern is established with reference air in one set of absorption cells and ozonized air in the other cell. After a time interval sufficient for the ozone distribution to reach equilibrium (about 30 seconds) the photo-detectors begin to record the signal intensity through each cell. The digitized signals are accumulated in the appropriate scalers and the total counts the transferred to the computer for storage on magnetic tape. A pair of solenoid valves (Fig. 1) is next activated by the computer to interchange the flow pattern in the absorption cells. During all the intervals while waiting for equilibrium to be achieved, pressure and temperature readings are made and updated frequently and transferred to the computer for storage. Then the transmittance signals are recorded and stored and again the flows are interchanged. After another equilibrium interval the signals are recorded and stored as previously. The three sets of measurements provide two determinations of the sample transmittance according to the procedure shown in Figure 2. The computer performs this process and computes the cross-section for the wavelength at which these data have been taken and stores the results on magnetic tape. When this process has been completed the computer signals the stepping motor controller to move the spectrometer drive to the next observation wavelength (in this case the wavelength step used is 0.05 nm) and the entire measurement sequence begins again.

2. Post-measurement data processing.

Following completion of a measurement run the data tapes are read into a larger computer system for more extensive processing.

This processing consists of: checking for outliers; recomputation of the cross sections with appropriate corrections; sorting the data into convenient logical wavelength blocks; averaging spectra of similar temperature; generation of temperature coefficients and a variety of plotting and printing functions.

The transmittances of the various cell pairs were computed according to Fig. 2. When the ozone concentration was sufficient so that the transmittance of the 5 cm assay cells dropped below 1% the processing used concentration data only from the 1 cm cells. Similarly, if the ozone concentration was low enough to cause the transmittance of the 1 cm cells to exceed 99% the processing used ozone concentration data only from the longer cells.

Three types of corrections to the data were included in the data processing. The first of these resulted from the fact that the cross-sections measured early in the measurement program relied on Vycor lamp envelopes and solar blind vacuum photodiodes to isolate the 253.65 nm Hg line in the assay cells. This combination was not ideally monochromatic. Later experiments showed that a 1% correction must be made to concentrations derived from early measurements to compensate for the lack of monochromaticity.

A second correction was made to account for the pressure distribution present in the flowing gas system. The pressure is slightly greater in the upstream assay cell than in the rest of the system. The correction resulted in a change of 0.2%.

The third correction was made to account for window reflections in the instrument. The correction was made by modelling the instrument with the assumptions: 1) each window had a reflectivity of 8%; 2) the windows were parallel; 3) the beam divergence was limited by the aperture of the detector

The resulting correction to the computed absorbance was fitted (2nd or 3rd order polynomial) to the transmittance for each of the 3 pairs of cells.

The above corrections tended to offset each other (lack of monochromaticity caused low estimates of the concentration while window reflections caused high estimates of the concentrations) so that the overall correction was typically less than 1% and in extreme cases reached only about 1.4%.

The data were extensively examined for internal consistency. Cross-sections determined from half-cycles 1 and 2 were compared with cross sections determined from half-cycles 2 and 3. Means and standard deviations of concentrations, transmittances, and other variables were computed for each run to verify the reproducibility of the measurements. Examination of these checks generally supports the conclusion that the system has approximately a 1% random noise in the determination of the cross sections.

One measure of the reliability of the data is the ability to reproduce the same values for the cross sections at the Hg line wavelengths when scanning using a continuum source and when making measurements using a Hg lamp. This tests both the photometric reproducibility of the system and the wavelength calibration since some of the lines (notably, the 334.15 nm line) occur at rapidly changing portions of the spectrum. Table I shows our scan data (continuum source) vs our line data (Hg source), and also gives Hearn's values for comparison.

Table I
Cross Sections at Selected Hg Lines (x 10^{19} cm^2)

		Hearn	Bass-Paur	
		Hg line	Hg line	Continuum
Hg line	T(C)	source	source	source
253.65	25	114.7	--	--
	-45		--	--
289.36	25	14.7	15.01	15.03
	-45		14.23	14.37
296.73	25	5.97	6.07	6.11
	-45		5.59	(5.66)*
302.15	25	2.86	2.94	2.98
	-45		2.64	(2.68)*
334.15	25	0.043	0.047	0.047
	-45		0.035	0.032

*Values computed from quadratic coefficients in absence of measured values.

References:

1. A. G. Hearn, Proc. Phys. Soc., 78, 932 (1961)

2. J. M. Bridges and W. R. Ott, Appl. Opt. 16, 367 (1977).

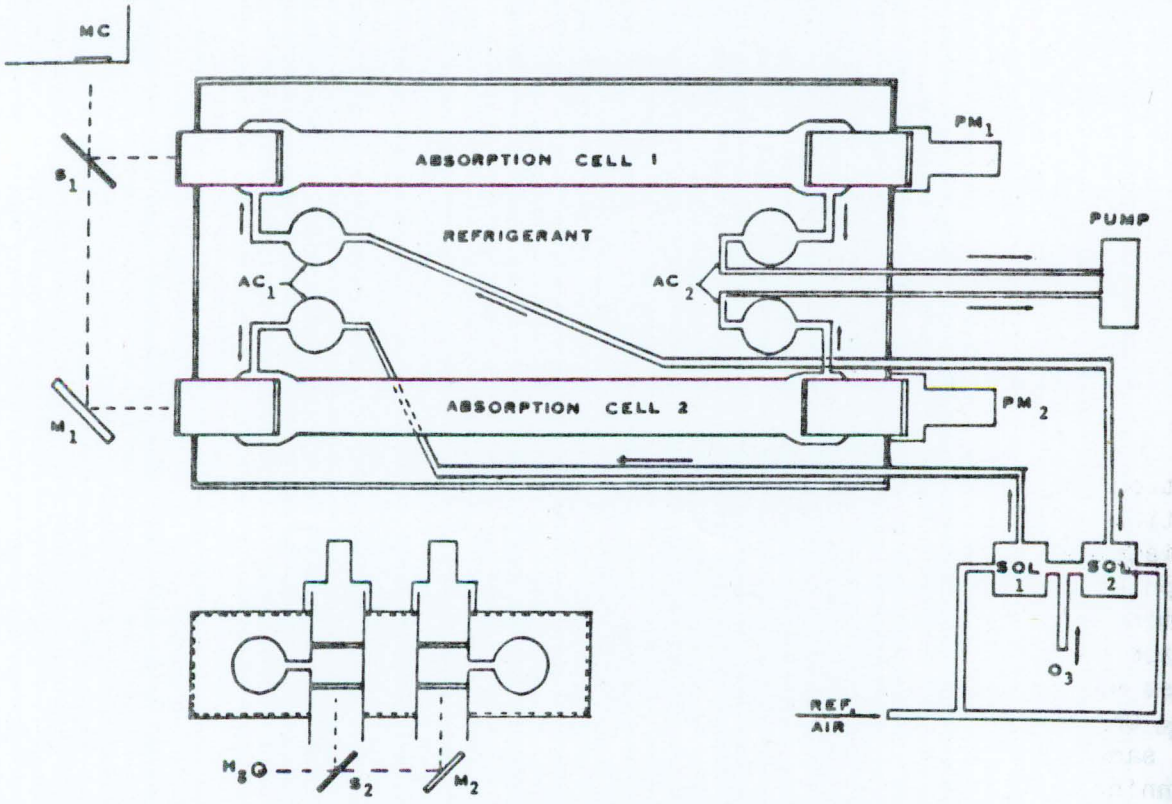

Schematic diagram of system for ozone cross-section measurements

Figure 1

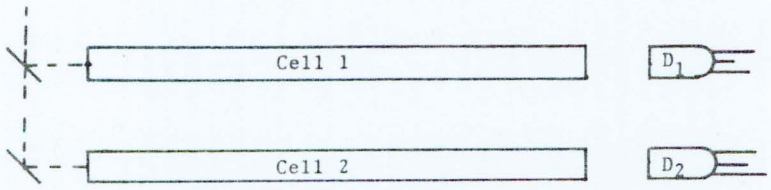

	cell 1	cell 2	
gas	REF	O_3 + REF	One
T_{freq}	$f_1(nom)$	$f_2(nom) \times T_{cell\ 2}$	half
ratio 1	$\frac{f_2(nom) \times T_{cell2}}{f_1(nom)}$		cycle

gas	O_3+REF	REF	Other
T_{freq}	$f_1(nom) \times T_{cell\ 1}$	$f_2(nom)$	half
Ratio 2	$\frac{f_2(nom)}{f_1(nom) \times T_{cell\ 1}}$		cycle

$$RATIO = \frac{Ratio\ 1}{Ratio\ 2} = \frac{f_2(nom) \times T_{cell\ 2}}{f_1(nom)} \times \frac{f_1(nom) \times T_{cell\ 1}}{f_2(nom)} = T_{cell\ 1} \times T_{cell\ 2} = Transmittance$$

Determination of transmittance of ozone sample

Figure 2

THE ULTRAVIOLET CROSS-SECTIONS OF OZONE: II. RESULTS AND TEMPERATURE DEPENDENCE

R. J. Paur, EPA*, Research Triangle Park, NC 27711
A. M. Bass, NBS**, Washington, DC 20234

Summary

Tables of ozone absorption cross-section in the ultraviolet have been prepared for intervals of 0.05 nm over the range 245 to 340 nm. At each wavelength entry in the table a set of coefficients has been derived that permits the cross-section to be computed as a function of temperature, between 200 K and 300 K, with an accuracy of 1%.

1. Temperature Dependence of the Cross-Section

As described in the preceding paper, ultraviolet absorption measurements of ozone were made at several temperatures in the range 200 to 300 K. The measurement temperatures were selected to be those most useful in atmospheric applications (-70, -55, -45, -30, 0, +25C). However, in order to extend the utility of these data we attempted to characterize quantitatively the nature of the temperature dependence of the ozone cross-sections. This was done by selecting several fixed wavelengths and by making measurements of the cross-sections at those wavelengths as the sample temperature was changed. We controlled the rate of cooling or warming of the system between 200 and 300 K so that we could measure the slowly changing cross-sections at three-minute intervals over a twelve to eighteen hour period. These temperature scans typically included 200-400 individual determinations, and were made for nine different wavelengths.

A plot of cross-section versus temperature for each of these measurements clearly shows curvature. A quadratic function was found to fit the data very well (Fig. 1). This observation is an agreement with the behavior of the temperature dependence as reported by Barbier and Chalogne (1) and forms the basis for the treatment of the temperature dependence of the entire absorption spectrum.

2. Computation of the Quadratic Coefficients

The cross sections were measured in assorted wavelength blocks as described in the preceding paper. The data were compiled into logical wavelength blocks of 5 nm and the spectra were then submitted to a two-pass filter which rejected outliers based on the amplitude of the cross sections and the noise in the data set at each wavelength. Following filtering of the data by the computer the data were plotted on a CRT for visual inspection; the operator was able to reject individual points or entire runs during the inspection procedure. Some of the spectra were

* Any policy issues discussed should not be construed to represent EPA policy.

**Work supported in part by the NASA Upper Atmosphere Program.

quite noisy; the filter was designed to reject entire runs if more than 20% of the individual points were rejected. The second pass through the filter was identical to the first except that the tolerance band was reduced by more than a factor of two. Less that 5% of the total data set was rejected.

The average spectrum at each of the six measurement temperatures was obtained by averaging all spectra of the reported temperature plus or minus 2 degrees.

Quadratic coefficients for the following equation were computed at each wavelength:

$$X\text{-sec} = C_o + C_1 * T + C_2 * T^2$$

where T is the temperature in degrees Celsius and X-sec is the cross section in units of 10^{-20} cm^2.

The quadratic coefficients were computed from all the available spectra. Thus the coefficients are temperature-weighted in proportion to the number of spectra at a given temperature. In some cases only 7 or 8 spectra were available; in other cases up to 30 spectra were available. Typically 14 to 18 spectra were used to determine the quadratic coefficients.

The accuracy of the quadratic model was computed for each 2.5 nm segment of the spectrum at each temperature. With few exceptions, the model agrees to within 1 percent of the measured values in the wavelength range from 245 to 330 nm.

At wavelengths longer than 330 nm the accuracy of the coefficients appears to deteriorate. In general this is due to a combination of less data and smaller cross sections. For example, in the range of 335 nm to 337.5 nm an average difference of less than 0.01 (less than 1 part in 10^5 of the cross section at 254 nm) leads to an error of more than 5 percent.

The average spectra and quadratic coefficients were printed along with data indicating the accuracy with which the synthetic spectra generated from the coefficients matched the measured spectra of various temperatures. A graphic presentation of the synthetic vs measured spectra is presented in Figure 2 for the wavelength range from 320 to 330 nm.

3. Temperature Dependence at 253.65 nm

As we have discussed previously, these measurements are based on the assumption that the ozone cross-section at 253.65 nm is not temperature-dependent. That assumption requires validation because if it is not correct then our low temperature values will have to be modified somewhat. The only published report on the temperature dependence of the ozone cross-section at this wavelength is that of Vigroux (2) which indicated that the cross-section decreases by 3% with the decrease in temperature between 18C and -75C.

We have made an effort to verify the nature of this relationship by inserting a second photometer in the ozone sample stream before the main photometer. The second photometer is an instrument that was designed to be the NBS laboratory standard for ozone calibrations, and is characterized by extremely good stability, sensitivity, and precision of measurement. It was found that when the two photometers were operated with the ozone sample at the same ambient temperature in both, they indicated essentially the same ozone concentration present in both photometers. However, when

the temperature of the cross-section photometer was reduced while the reference standard photometer was kept at room temperature, the cross-section photometer indicated an apparent increase in the ozone concentration. Since the same sample flows through both photometer and the concentration in the second photometer cannot increase, we believe this indicates an increase in the cross-section as the temperature is reduced. Our measurements suggest an increase of about 1.3% for a change in temperature from +25C to -70C. Some other recent measurements (3,4) also suggest that the cross-section actually increases with decreasing temperature.

Although our method of measurement is somewhat indirect, we believe that this effect is real. An absolute measurement of higher accuracy than previously achievable would be required to verify these observations on the temperature effect and to specify the magnitude of the effect more exactly. Therefore, we have not included any temperature effect for the 253.65 nm wavelength. If later measurements establish the magnitude for the temperature effect, a linear correction can be made to update the entire data set.

4. The Data Tables

Estimation of the overall accuracy of these measurements is not straightforward. The measurements use a value of $1147 \times 10^{-20} cm^2$ for the 254 cm cross section. It has been assumed that the value does not vary with temperature.

From the photometric precision of the instrument and the quality of agreement of the concentrations from the two pairs of assay cells, it appears likely that the concentration is measured to within 1%. From the photometric precision of the instrument and comparison of the cross section with the standard reference photometer for the assay of ozone it appears likely that the cross sections are measured to within 1%. Examination of the internal consistency of several sets of measurements at each of six temperature shows that for cross sections larger than 0.2×10^{-20} cm^2 the data lie within 1% of a model which assumes a (different) quadratic temperature dependence at each wavelength measured. This latter fact leads us to estimate that the relative cross sections are accurate to about 1% for the wavelength range 245 nm to 330 nm.

The results of this measurement program have been collected in a set of tables that provides cross-sections vs wavelength and temperature. The tables consist of two parts. (Figures 3 and 4 are sample pages from the tables.) In Part A the table entry contains the wavelength (in 0.05 nm intervals) and the value of the cross-section for each of the six measurement temperatures. In Part B the table entry contains the wavelength and the three coefficients that permit the cross-section to be computed for any temperature between 200 K and 300 K with an estimated accuracy of 1%.

References:

1. D. Barbier and D. Chalogne, Ann de phys. (11) 17, 272 (1942).
2. E. Vigroux, Ann physique 8, 709 (1953).
3. D. E. Freeman, unpublished results.
4. L. Molina, unpublished results.

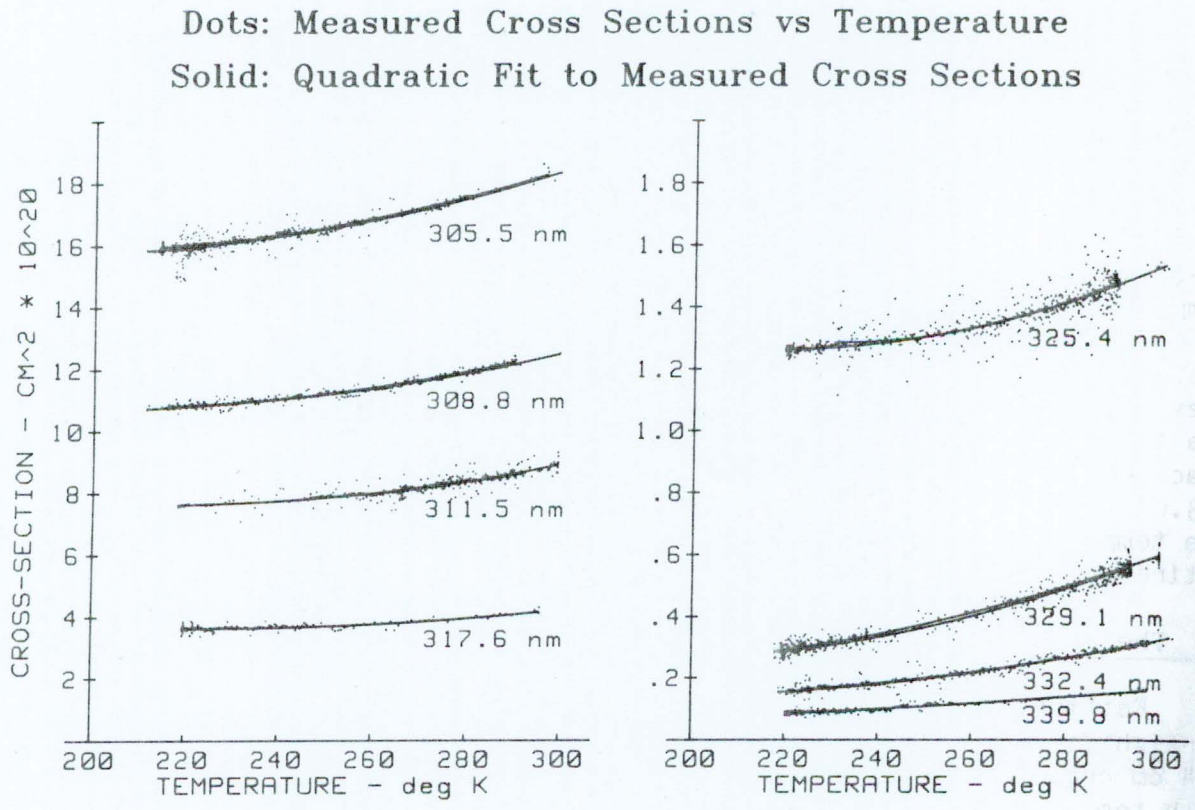

Figure 1

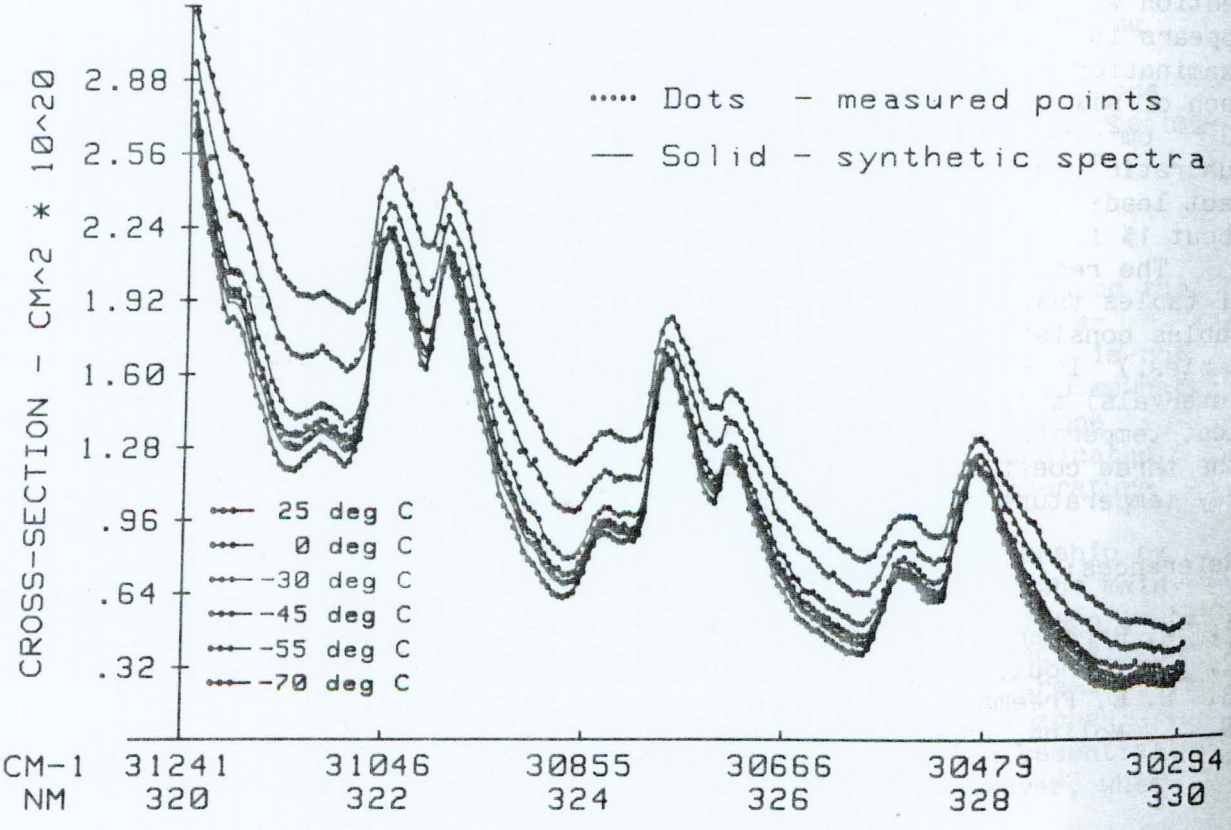

Figure 2

Ozone spectrum: 267.5 to 270.0 nm; Xsecs*10^20 cm^2 July 9,1984 Page 10A

NM (air)	CM-1(vac)	-70 C	-55 C	-45 C	-30 C	0 C	25 C
267.511	37370.5	887.39	889.95	---	892.73	883.11	885.22
267.561	37363.6	889.35	889.36	880.49	892.46	880.90	886.58
267.611	37356.6	---	886.93	887.29	889.29	878.94	886.07
267.661	37349.6	882.86	886.73	883.51	886.82	881.48	883.99
267.711	37342.6	881.64	884.36	881.90	877.58	875.38	881.37
267.761	37335.6	881.30	885.69	868.29	877.79	871.27	879.07
267.811	37328.7	875.10	876.64	872.43	879.32	870.70	876.40
267.861	37321.7	870.94	870.16	867.41	876.21	866.53	876.25
267.911	37314.7	863.01	873.77	858.30	867.88	865.91	870.23
267.960	37307.9	859.90	868.47	857.96	866.75	858.32	865.05
268.010	37301.0	857.15	864.81	---	862.06	854.49	861.94
268.060	37294.0	852.65	864.02	850.35	856.62	851.05	860.68
268.110	37287.0	841.17	847.50	850.79	849.32	842.60	855.83
268.160	37280.1	841.34	844.10	---	849.74	843.46	851.50
268.210	37273.1	837.64	842.17	846.17	845.68	839.83	846.32
268.260	37266.2	832.80	838.70	---	840.13	847.20	843.56
268.310	37259.3	830.32	829.32	828.51	836.97	839.81	839.56
268.360	37252.3	825.82	825.07	822.00	831.87	824.94	834.97
268.410	37245.4	818.13	820.80	819.54	825.43	824.41	829.70
268.460	37238.4	810.20	822.35	823.11	823.03	820.29	827.27
268.510	37231.5	814.92	819.38	824.20	821.27	819.83	826.28
268.560	37224.6	811.44	818.54	---	817.88	823.54	823.90
268.610	37217.6	810.90	821.23	813.08	819.73	809.62	820.98
268.660	37210.7	808.98	814.18	816.89	811.81	810.17	818.62
268.710	37203.8	805.62	808.81	810.31	811.45	809.47	815.13
268.760	37196.9	805.32	813.68	---	808.55	806.80	814.44
268.810	37190.0	801.56	806.72	809.90	804.84	803.58	812.41
268.860	37183.0	799.55	799.17	806.58	803.18	798.15	808.20
268.910	37176.1	792.37	796.24	805.04	799.69	797.16	806.16
268.960	37169.2	790.06	797.21	794.55	797.35	794.32	802.51
269.010	37162.3	791.17	794.21	796.12	796.21	794.93	800.90
269.060	37155.4	785.93	786.54	800.50	795.24	795.30	798.25
269.110	37148.5	785.38	791.63	789.49	790.03	789.99	797.22
269.160	37141.6	---	789.73	789.09	794.80	789.24	796.18
269.210	37134.7	788.55	796.92	803.63	795.05	794.04	797.61
269.260	37127.8	789.23	802.20	---	800.26	793.47	797.97
269.310	37120.9	790.39	796.99	800.77	798.62	798.71	799.21
269.360	37114.0	794.86	803.85	790.52	802.58	803.73	801.03
269.410	37107.1	798.95	807.90	807.81	809.30	801.57	804.94
269.460	37100.2	806.85	806.67	802.43	815.54	806.12	807.11
269.510	37093.4	806.63	810.49	811.86	817.50	804.37	808.23
269.560	37086.5	808.26	815.99	---	817.05	809.17	811.69
269.610	37079.6	813.05	816.60	815.10	---	807.68	811.54
269.660	37072.7	815.04	822.19	814.21	813.28	806.89	810.63
269.710	37065.9	816.43	813.39	805.82	---	805.55	810.69
269.760	37059.0	813.40	809.69	807.06	809.28	802.25	807.53
269.810	37052.1	804.43	806.56	806.17	807.16	804.24	809.72
269.860	37045.3	799.88	800.81	793.00	792.85	795.32	802.41
269.910	37038.4	797.24	801.86	785.84	787.43	790.38	798.50
269.960	37031.5	790.74	792.59	---	788.10	788.36	795.40

Fit of synthetic (quadratic coefs) spectra to measured average spectra

Aver difference	-1.90	2.30	-.21	1.74	-3.56	.54
Std dev of Dif	1.47	2.89	4.09	2.43	2.37	.36
100*AveDif/AveXS	-.23	.28	-.03	.21	-.43	.07